

# Monte Carlo modeling of electron beams from a NEPTUN IOPC medical linear accelerator

Nasrollah Jabbari,  
Bijan Hashemi-Malayeri

**Abstract.** The Monte Carlo (MC) simulation of radiation transport is considered to be one of the most accurate methods of radiation therapy dose calculation. With the rapid development of computer technology, MC-based treatment planning for radiation therapy is becoming practical. A basic requirement for MC treatment planning is a detailed knowledge of radiation beams of medical linear accelerators (linacs). A practical approach to acquire this knowledge is to perform MC simulation of radiation transport for linacs. The aims of this study were: modeling of the electron beams from the NEPTUN IOPC linear accelerator (linac) with the MC method, obtaining of the energy spectra of electron beams, and providing the phase-space files for the electron beams of this linac at different field sizes. Electron beams produced by the linac were modeled using the BEAMnrc MC system. Central axis depth-dose curves and dose profiles of the electron beams were measured experimentally and also calculated with the MC system for different field sizes and energies. In order to benchmark the simulated models, the percent depth dose (PDD) and dose-profile curves calculated with the MC system were compared with those measured experimentally with diode detectors in an RFA 300 water phantom. The results of this study showed that the PDD and dose-profile curves calculated by the MC system using the phase-space data files matched well with the measured values. This study demonstrates that the MC phase-space data files can be used to generate accurate MC dose distributions for electron beams from NEPTUN IOPC medical linac.

**Key words:** Monte Carlo • radiotherapy • electron beams • linac

N. Jabbari  
Department of Medical Imaging,  
Urmia University of Medical Sciences,  
Urmia, Iran

B. Hashemi-Malayeri✉  
Department of Medical Physics,  
Faculty of Medical Sciences,  
Tarbiat Modares University,  
Ale-Ahmad and Chamran Cross,  
Tehran 1411713116, Iran,  
Tel.: +98 21 828 83892, Fax: +98 21 880 06544,  
E-mail: bijanhashemi@yahoo.com

Received: 6 October 2008  
Accepted: 3 August 2009

## Introduction

Electron beam radiation therapy is used extensively for treating head and neck cancers to avoid the irradiation of the spinal cord. It is also used for treating chest wall malignancies to limit the irradiated volume of lungs. Calculating the dose distribution from an electron field is quite complicated because of the multiple scattering, especially in the presence of internal heterogeneities [18]. The Monte Carlo method can precisely model the physical processes involved in radiation therapy and is powerful in dealing with any complex geometry [15]. Ever since the first appearance of Monte Carlo techniques in radiotherapy physics, physicists have been making steady progress towards full-scale treatment planning using a Monte Carlo dose engine [21]. The currently available commercial systems for electron treatment planning are associated with large uncertainties, especially in irradiated volumes containing inhomogeneities such as air cavities and bones. The Monte Carlo method is generally considered to be the most accurate approach for electron dose calculation under all circumstances [13, 16].

A Monte Carlo treatment planning system needs detailed information about the beams incident on the

patient. In order to initiate the transport of particles in the patient CT model, accurate phase-space information about the particles on the patient surface is required. This information includes the energy, angular, and spatial distributions of the particles in the clinical electron beams [19]. Direct measurement of this information for a clinical beam is very difficult, if not impossible, due to the very high radiation intensities encountered in clinical beams [3]. On the other hand, calculation of beam phase-space parameters using analytical methods is not flexible and usually employs approximations [5, 12]. However, a method used for determining the initial phase space (IPS) of a clinical electron beam is to simulate the electron transport through the head of a clinical linac and register the electrons that enter the IPS plane [11]. The EGS4/BEAM Monte Carlo code system is an implementation of this method [21]. Therefore, the most practical way to obtain detailed information about the incident radiation beam is regarded to be the Monte Carlo simulation of the treatment head [1, 4, 6, 17].

The aims of this study were: modeling the electron beams of the NEPTUN 10PC linac with MC method, obtaining the energy spectra of electron beams, and providing the phase-space files for the electron beams of this linac at different field sizes.

## Material and methods

### Medical linear accelerator

In this study, all experimental measurements and Monte Carlo calculations were performed on a NEPTUN 10PC medical linac. This is a stationary wave type linac equipped with an achromatic bending magnet system. This linac provides both photon and electron beams. In this investigation, all the linac electron beams (6, 8 and 10 MeV) were studied. In the electron beam mode, the primary electrons impinge on one of two available scattering foils (one for the 6 and 8 MeV and another for the 10 MeV electron beams). These foils are made from different thicknesses of lead. The appropriate scattering foil is automatically selected for a particular nominal energy.

The X-ray jaws provide the first collimation for the broad electron beam. The electron beams coming through the X-ray jaws are of uniform intensity distribution. There are two sets of trimmers, one for the fields smaller than  $10 \times 10 \text{ cm}^2$  and another for the fields larger than  $10 \times 10 \text{ cm}^2$ . The trimmers have only to progressively collimate the beam using a set of five aperture plates without the use of any wall scatter. These aperture plates have decreasing dimensions downstream. The bottom aperture plate defines the treatment field size. The combination of trimmers with photon jaws provides electron beams with different field sizes ranged from  $3 \times 3 \text{ cm}^2$  up to  $25 \times 25 \text{ cm}^2$ .

### Experimental measurements

The linac electron energy is typically determined from the measurements of the practical range in a water

phantom. The most probable electron energy at the phantom surface  $E_{p_0}$  can be determined from the depth of the practical range  $R_p$  in water using the following equation [2]:

$$(1) \quad E_{p_0} = 0.22 + 1.98R_p + 0.0025R_p^2$$

Another energy of interest for calibration purposes is the average energy on the phantom surface, which can be determined from the  $R_{50}$ , the depth at which the dose falls to 50% of the maximum dose, using the following equation [15]:

$$(2) \quad E_0 = 2.33R_{50}$$

Although the linac manufacturers state nominal electron energies, the central axis percent depth dose (PDD), characteristics of electron beams, are really the parameters of clinical interest [7].

Central axis depth-dose curves were measured in water at SSD = 100 cm using a computerized water phantom (Scanditronix RFA-300<sup>1)</sup>) radiation field analyzer, which is a dosimetry system for the 3D radiation field analysis. A waterproof high-doped p-type silicon diode (EFD-3G), made by the same manufacturer was used to measure the percentage depth doses at the central axis. The thickness of this silicon chip is 0.5 mm and its active area diameter is 2 mm. Another diode was placed in the periphery of the radiation field during the experimental measurements, as the reference detector. The PDD curves for 6, 8 and 10 MeV electron beams were measured with trimmers in the place for three field sizes ( $3 \times 3$ ,  $10 \times 10$ ,  $25 \times 25 \text{ cm}^2$ ) at SSD = 100 cm using the IAEA protocol [8]. In addition, the dose profiles were measured for the reference field size ( $10 \times 10 \text{ cm}^2$ ) at the  $d_{\text{max}}$  for each electron beam. All the curves were plotted from the average values obtained from three separate measurements made for every situation.

### Monte Carlo calculations

The electron beams were modeled using the BEAM-nrc system [22] based on EGSnrc code [14]. Detailed information regarding the geometry and material of various components of the treatment head, required for the Monte Carlo simulation of the linac machine (NEPTUN 10PC), was provided by the vendor<sup>2)</sup>. The geometry of the linac treatment head structure was modeled for three field sizes ( $3 \times 3$ ,  $10 \times 10$  and  $25 \times 25 \text{ cm}^2$ ) and three nominal electron beam energies (6, 8 and 10 MeV) at SSD = 100 cm. All the simulations required for investigating the PDD curves and dose profiles of the three nominal electron beam energies (6, 8, and 10 MeV) were performed with monoenergetic point sources being generated by the linac. The BEAMnrc was run under the Microsoft Windows XP<sup>®</sup> operating system using a dual processor (3800 GHz, ADM Athlon<sup>™</sup>,  $64 \times 2$  Dual Core Processor, 1 GB RAM) computer.

<sup>1)</sup> IBA Scanditronix Medical AB, Uppsala, Sweden.

<sup>2)</sup> ZDAJ IPJ Świerk, NEPTUN 10PC technical and operational documentation. Hungary 1996.

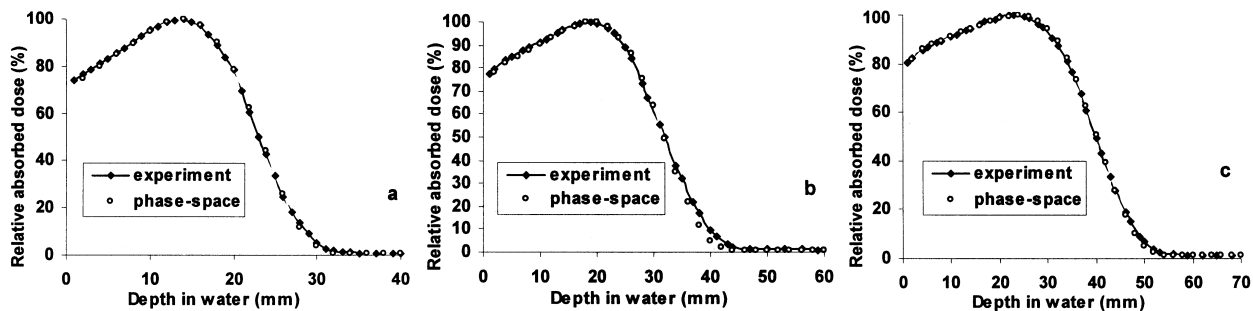


**Fig. 1.** Central axis PDD curves derived from the experimental measurements and MC calculations (from the phase-space files) for different electron beam energies of the NEPTUN 10PC linac: 6 MeV (a), 8 MeV (b) and 10 MeV (c), at the reference field size ( $10 \times 10 \text{ cm}^2$ ).

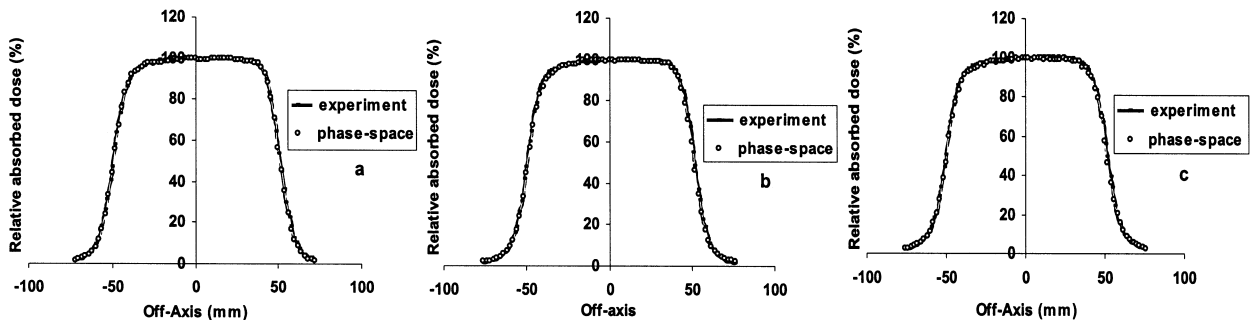


**Fig. 2.** Dose profiles derived from the experimental measurements and MC calculations (from the phase-space files) for different electron beam energies of the NEPTUN 10PC linac: 6 MeV (a), 8 MeV (b) and 10 MeV (c), at the reference field size ( $10 \times 10 \text{ cm}^2$ ).

The electron beam energies were adapted to give the depth-dose curves having the same depth at the 50% dose level. In all of the simulations, the energy cut-offs for particle transport were set at  $ECUT = 0.7 \text{ MeV}$  (kinetic energy plus rest mass) and  $PCUT = 0.010 \text{ MeV}$  for the electrons and photons, respectively.

Sufficient histories were followed to achieve a precision better than 1% for the calculation of dose distributions for the linac electron beams. In the BEAMnrc code, the particles, after transporting, were scored at a scoring plane placed after the last scraper. The information of this scoring plane, which is named the phase-space file, was used as the source input for the simulations of the dose distributions in a rectilinear voxel geometry water phantom using the DOSXYZnrc system [23], which is also based on the EGSnrc code. The depth dose and dose-profile values from the phase-space files for three electron beams were calculated in the simulated water phantom using the DOSXYZnrc code.

In order to benchmark the simulated models, the PDD curves and dose profiles at  $d_{max}$  were also measured experimentally for all the energy settings at the reference field size with the diode detectors in the RFA 300 water phantom, as mentioned above. Then, the calculated values, estimated by the MC method, were compared and tested against the measured values using the Kolmogorov–Smirnov statistical test.

After the benchmarking of the simulated machine for the three electron beam energies (6, 8 and 10 MeV), at the reference field size, the most probable electron energy at the phantom surface  $E_{p0}$  and the average energy on the phantom surface  $E_0$  were obtained from the measured and calculated data using Eqs. (1) and (2). In addition, the central axis depth-dose curves of the electron beams for the smallest and largest field sizes

( $3 \times 3 \text{ cm}^2$  and  $25 \times 25 \text{ cm}^2$ ) were measured and calculated. Then, the measured and calculated values of the PDD curves were compared with each other.

The energy spectra of the electron beams were compiled from the phase-space files in a scoring plane of the BEAMnrc code using the computer code BEAMDP [20]. The energy bin size was set at 0.1 MeV intervals for the calculation of energy spectra.

## Results

Figure 1 shows the measured and calculated depth-dose curves for the linac electron beams (6, 8, and 10 MeV) in the reference field ( $10 \times 10 \text{ cm}^2$ ). Figure 2 shows the dose profiles measured and calculated at the  $d_{max}$  for the three electron beam energies at the reference field.

Table 1 shows the  $P$ -values of the Kolmogorov–Smirnov test resulted from the comparison of the calculated values of the PDD and dose profile with the experimental ones. The Kolmogorov–Smirnov test indicated that the PDD and the dose profiles calculated with the MC code match well with those measured, everywhere on the curves for all the linac electron beams.

**Table 1.** The  $P$ -values of the K-S test resulted from the comparison of the data derived from the experimental measurements and the MC calculations for the reference field size

Electron beam energy (MeV)	PDD $P$ -values	The dose profile $P$ -values
6	0.819	0.416
8	0.358	0.759
10	0.346	0.769

**Table 2.** The measured and calculated values of the  $E_{p0}$  for the three electron beams of the linac

Electron beam energy (MeV)	Measured value	Calculated value
6	$6.21 \pm 0.02$	$6.20 \pm 0.01$
8	$8.24 \pm 0.06$	$8.25 \pm 0.01$
10	$9.94 \pm 0.02$	$9.93 \pm 0.01$

**Table 3.** The measured and calculated values of the  $E_0$  for the three electron beams of the linac

Electron beam energy (MeV)	Measured value	Calculated value
6	$5.68 \pm 0.02$	$5.67 \pm 0.01$
8	$7.44 \pm 0.03$	$7.45 \pm 0.01$
10	$9.29 \pm 0.01$	$9.30 \pm 0.01$

Tables 2 and 3 show the values of the most probable electron energy at the phantom surface  $E_{p0}$  and the average energy on the phantom surface  $E_0$  obtained from the measured and calculated data using Eqs. (1) and (2) for the three electron beam energies at the reference field size.

Figures 3 and 4 show the measured and calculated depth-dose curves obtained for the 6, 8, and 10 MeV

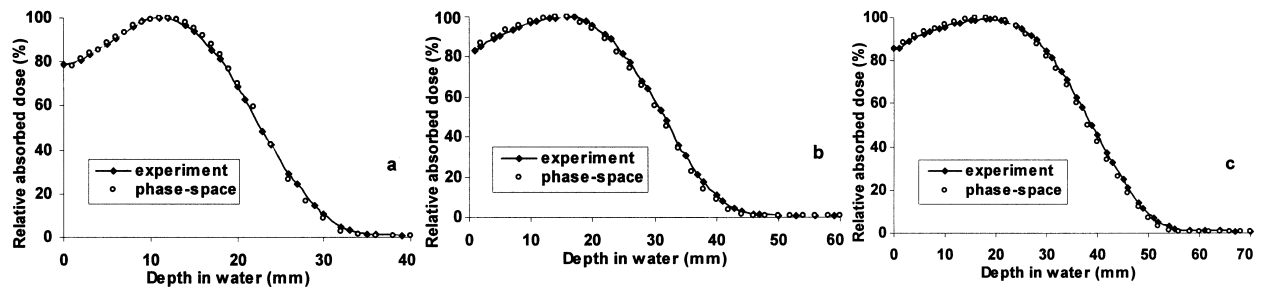
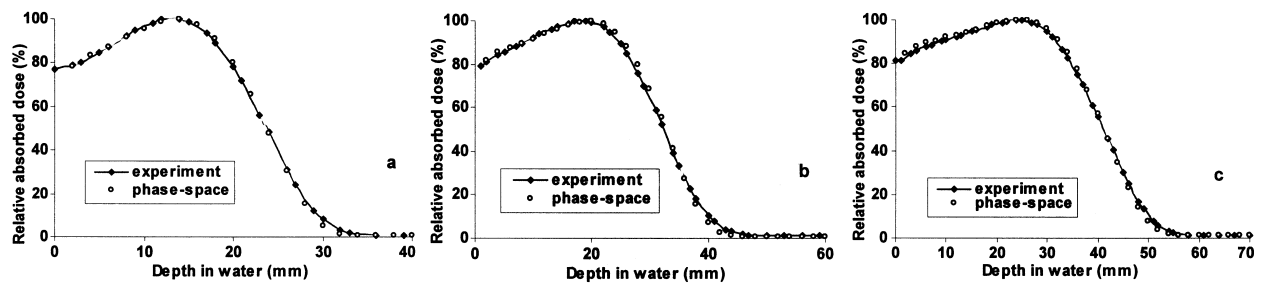
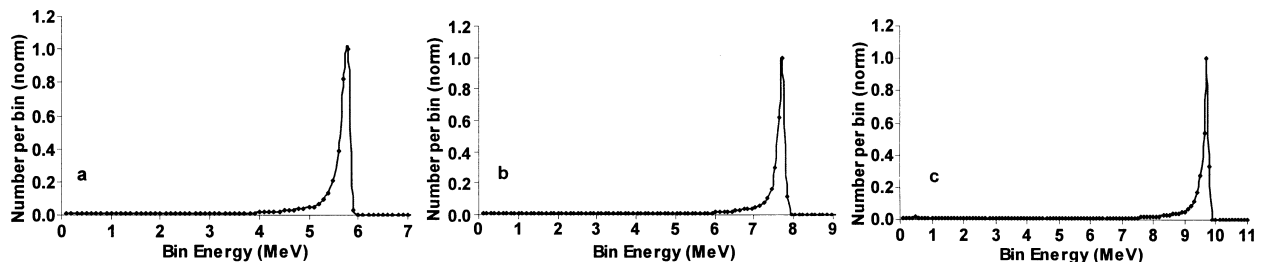
**Table 4.** The  $P$ -values of the K-S test resulted from the comparison of the PDD calculated values with the experimental ones for the smallest ( $3 \times 3 \text{ cm}^2$ ) and largest ( $25 \times 25 \text{ cm}^2$ ) field sizes

Electron beam energy (MeV)	PDD $P$ -value for the smallest field size	PDD $P$ -value for the largest field size
6	0.621	0.415
8	0.387	0.215
10	0.918	0.171

electron beams in the smallest ( $3 \times 3 \text{ cm}^2$ ) and largest ( $25 \times 25 \text{ cm}^2$ ) field sizes.

Table 4 shows the  $P$ -values of the Kolmogorov–Smirnov test resulted from the comparison of the PDD calculated values with the experimental ones for the smallest ( $3 \times 3 \text{ cm}^2$ ) and largest ( $25 \times 25 \text{ cm}^2$ ) field sizes. The Kolmogorov–Smirnov test indicated that the PDD values calculated with the MC code match well with those measured, everywhere on the curves for all the electron beams.

The electron energy spectra for the monoenergetic initial beams from the MC code at the reference field size at a scoring plane after the last scraper are shown in Fig. 5. All the spectra curves are normalized to their most probable energy.

**Fig. 3.** Central axis PDD curves derived from the experimental measurements and MC calculations (from the phase-space files) for different electron beam energies of the NEPTUN 10PC linac: 6 MeV (a), 8 MeV (b) and 10 MeV (c), at the smallest field size ( $3 \times 3 \text{ cm}^2$ ).**Fig. 4.** Central axis PDD curves derived from the experimental measurements and MC calculations (from the phase-space files) for different electron beam energies of the NEPTUN 10PC linac: 6 MeV (a), 8 MeV (b) and 10 MeV (c), at the largest field size ( $25 \times 25 \text{ cm}^2$ ).**Fig. 5.** The electron beam energy spectra after the last scraper for the three electron beam energies, 6 MeV (a), 8 MeV (b) and 10 MeV (c), at the reference field size.

## Discussion

In this study the measured doses in homogeneous media exposed to electron beams (6, 8 and 10 MeV) were compared to those predicted by the EGSnrc Monte Carlo code. The study was facilitated by the availability of the BEAMnrc system, based on EGSnrc code, to perform full, 3D, treatment head simulations and to get phase-space output data, giving a more detailed description of electron beams. The main objective of BEAMnrc calculations in this study was to generate a variety of phase-space data files to be used as input source files for the DOSXYZnrc program to calculate dose distributions in a water phantom. Other important goals of this study were to improve our understanding of some commonly used clinical electron beams and use this information to provide robust beam models having little impact on the accuracy of dose calculations. We focused on one typical linear accelerator, NEPTUN 10PC, using scattered beams. The methodology employed in this research is generally applicable to any accelerator and all particles (electrons, positrons, and photons) for both of the clinical electron and photon beams.

The results of this study showed that the Monte Carlo calculations using the phase-space data files match well with the measured PDD and dose-profile curves (within 2%). Our findings also indicated that the agreement between the values of the most probable electron energy at the phantom surface  $E_{p0}$  and the average energy on the phantom surface  $E_0$  obtained from the measured and calculated data is very good (within 1%) in most cases. These prove the validity of the Monte Carlo simulation method used in this study for the determination of the initial phase-space data files.

Ma and Jiang [19] found that the Monte Carlo simulation of radiation transport is one of the most accurate methods for predicting absorbed dose distributions in radiation therapy. A Monte Carlo treatment planning system needs detailed information about the beams incident on the patient [9]. The only method to obtain accurate electron beam phase-space information is to simulate the accelerator treatment head using the Monte Carlo method already being pointed out by Jiang *et al.* [13].

The energy spectra for each electron beams were derived from the simulated phase-space data files using the computer code BEAMDP [20]. The beam characteristics are usually different due to the variation in accelerator designs and on-site beam tuning. It was noted that the energy spectra at the scoring plane after the last scraper obtained by the MC method for the linac, NEPTUN 10PC, have fewer low-energy electrons. This can be explained by the fact that the energy spectra at the scoring plane are strongly dependent on the details of the accelerator tube tuning characteristic being already pointed out by Jabbari *et al.* [10]. Furthermore, Deasy *et al.* [3] and Kok and Welleweerd [16] have also found that the energy spectra are only moderately affected by the scattering foil design, as the scattering foil thickness cannot account for the measured spectral width or its shape.

## Conclusion

This study demonstrated that the phase-space data files can be used to generate accurate MC dose distributions for electron beams from a NEPTUN 10PC linac. The phase-space data can be used as input to calculate dose distributions in a patient's CT phantom. Monte Carlo calculations of dose distribution using multiple-source models is an alternative to using the phase-space information as direct input to the dose calculation code. Further studies are required to realize the full potential of the multiple-source models from NEPTUN 10PC linac for Monte Carlo treatment planning.

**Acknowledgment.** The authors would like to thank the head and staff of the Radiotherapy Department of Imam-Khomein Hospital of Tabriz for their help and technical assistance in performing experimental measurements on their Neptun 10PC linac machine. The authors would also like to appreciate the ZDAJ Company for providing the detailed information and technical specifications of NEPTUN 10PC linac used for the Monte Carlo simulation in this study.

## References

- Balog JP, Mackie TR, Wenman DL, Glass M, Fang G, Pearson D (1999) Multileaf collimator interleaf transmission. *Med Phys* 26:176–186
- Bjork P, Knoos T, Nilsson P (2002) Influence of initial electron beam characteristics on Monte Carlo calculated absorbed dose distributions for linear accelerator electron beams. *Phys Med Biol* 47:4019–4041
- Deasy JO, Almond PR, McEllistrem MT (1996) Measured electron energy and angular distributions from clinical accelerators. *Med Phys* 23:675–684
- DeMarco JJ, Solberg TD, Smathers JB (1998) A CT-based Monte Carlo simulation tool for dosimetry planning and analysis. *Med Phys* 25:1–11
- Desobry GE, Boyer AL (1994) An analytic calculation of the energy fluence spectrum of a linear accelerator. *Med Phys* 21:1943–1952
- Faddegon B, Balogh J, Mackenzie R, Scora D (1998) Clinical considerations of Monte Carlo for electron radiotherapy treatment planning. *Radiat Phys Chem* 53:217–227
- Followill DS, Davis DS, Ibbott GS (2004) Comparison of electron beam characteristics from multiple accelerators. *Int J Radiat Oncol Biol Phys* 59:905–910
- IAEA (2000) Absorbed dose determination in external beam radiotherapy. IAEA Technical Reports Series no. 398. International Atomic Energy Agency, Vienna
- Jabbari N, Hashemi-Malayeri B, Farajollahi A, Kazemnejad A (2007) Monte Carlo calculation of scattered radiation from applicators in low energy clinical electron beams. *Nukleonika* 52:97–103
- Jabbari N, Hashemi-Malayeri B, Farajollahi A, Kazemnejad A, Shafae A, Jabbari S (2007) Comparison of MCNP4C and EGSnrc Monte Carlo codes in depth-dose calculation of low energy clinical electron beams. *J Phys D: Appl Phys* 40:4519–4524
- Janssen JJ, Korevaar EW, Van Battum LJ, Storch PRM, Huizenga H (2001) A model to determine the initial phase space of a clinical electron beam from measured beam data. *Phys Med Biol* 46:269–286

12. Jeraj R, Keall PJ, Ostwald PM (1999) Comparisons between MCNP, EGS4 and experiment for clinical electron beams. *Phys Med Biol* 44:705–717
13. Jiang SB, Kapur A, Ma CM (2000) Electron beam modeling and commissioning for Monte Carlo treatment planning. *Med Phys* 27:180–191
14. Kawrakow I, Rogers DWO (2006) The EGSnrc Code System: Monte Carlo simulation of electron and photon transport. NRCC Report PIRS-701. NRCC, Ottawa
15. Khan FM, Doppke KP, Hogstrom KR *et al.* (1991) Clinical electron-beam dosimetry: report of AAPM Radiation Therapy Committee Task Group no. 25. *Med Phys* 18:73–109
16. Kok JG, Welleweerd J (1999) Finding mechanisms responsible for the spectral distribution of electron beams produced by a linear accelerator. *Med Phys* 26:2589–2596
17. Lee PC (1997) Monte Carlo simulations of the differential beam hardening effect of a flattening filter on a therapeutic X-ray beam. *Med Phys* 24:1485–1489
18. Ma CM, Faddegon BA, Rogers DWO, Mackie TR (1997) Accurate characterization of Monte Carlo calculated electron beams for radiotherapy. *Med Phys* 24:401–416
19. Ma CM, Jiang SB (1999) Monte Carlo modeling of electron beams from medical accelerators. *Phys Med Biol* 44:R157–R189
20. Ma CM, Rogers DWO (2007) BEAMDP users manual. NRCC Report PIRS-0509C (rev. A). NRCC, Ottawa
21. Rogers DWO, Faddegon BA, Ding GX, Ma CM, We J, Mackie TR (1995) BEAM: a Monte Carlo code to simulate radiotherapy treatment units. *Med Phys* 22:503–524
22. Rogers DWO, Walters B, Kawrakow I (2007) BEAMnrc users manual. NRCC Report PIRS-0509 (A). NRCC, Ottawa
23. Walters B, Kawrakow I, Rogers DWO (2006) DOSXYZnrc users manual. NRCC Report PIRS-794 (rev. B). NRCC, Ottawa